

# Numerical Simulation of Laminar Flow Above and Below Triangular Bedforms

C. Gualtieri

University of Napoli Federico II, Napoli (Italy)

Via Claudio 21, 80125, Napoli (Italy), carlo.gualtieri@unina.it

**Abstract:** This paper presents some results of numerical simulations carried out to investigate the basic hydrodynamic interactions between the laminar flow in the water column above triangular bedforms and the Darcian flow in the underlying permeable sediments. The flow was described by the Navier-Stokes equation in the free region and the Darcy equation in the porous region. Numerical simulations were carried out in laminar steady-state flow using Multiphysics 3.5a in a range of bedforms height-based Reynolds number  $Re_H$  from 6 to 3852. Numerical results confirmed the close relationship between the characteristics of the separation region in the water column downstream the bedform crest and those of the hyporheic zone in the porous medium.

**Keywords:** Environmental hydraulics, laminar flow, bedforms, porous media.

## 1. Introduction

Despite the traditional separation between the studies of surface water and groundwater flows, since some decades it has been recognized that rivers and aquifers are strongly connected and their interaction gives rise to a continuous exchange of water and solutes, which exerts a significant influence on the water quality (Bencala and Walters, 1983). This analysis led to identify a zone, termed *hyporheic zone*, where groundwater and stream water are mixing. The hyporheic zone has hydrodynamical, physiochemical and biotic characteristics different from both the river and the subsurface environments (Dade, 1993, Boulton et al., 1998) and controls the distribution of solutes, colloids, dissolved gases and biogeochemical reactions from ripple to global scales (Huettel et al., 1998, 2003; Nishihara and Ackerman, 2008), and thus affects the distribution of benthic flora and fauna in lakes, oceans, bays and estuaries, as well as hyporheic and riparian organisms in fluvial systems (Findlay, 1995; Brunke and Gonser, 1997). The effects of the hyporheic exchange

processes on both the river and the subterranean environments are twofold. First, the hyporheic zone acts as a storage zone or a dead zone, which temporarily traps stream-transported solutes and then releases them after some time. Due to the low filtration velocities in the subsurface, the residence time of solutes in the hyporheic zone is usually much longer than the travel time in the main stream. This difference between the characteristic timescales of in-stream and hyporheic flow determines long tails in the time-concentration curves (Bencala and Walters, 1983, Wörman et al., 2002). Second, the metabolic activity of the hyporheic microorganisms significantly alters the in-stream concentration of chemicals, both at the reach scale (Findlay et al., 1993) and at the basin scale (Harvey and Fuller, 1998). The surface of the hyporheic sediments is covered by biofilms of aerobic microorganisms, that use the dissolved oxygen from the surface water to oxidize nitrogen and phosphorus for their metabolism (Boulton et al., 1998; Hancock et al., 2005). The hyporheic exchange is also important for riparian vegetation, as the oxygen flux from the stream regulates the redox conditions in the aquifer and therefore the dynamics of nutrients and trace metals (Brunke and Gonser, 1997).

Examples of vertical, lateral and longitudinal hyporheic exchange processes between a river and its surrounding groundwater are presented in Fig.1.

Different approaches were proposed to study surface water-groundwater interactions and the hyporheic zone, as pointed out by Boano (2006). First, a number of studies relied on detailed field measurements of the topographical and hydraulic features of specific sites in order to calibrate 2D or 3D numerical groundwater flow models. This approach allows hyporheic paths to be modelled, and the interactions between the hyporheic zone and the surrounding aquifer to be described at scales of the order of hundreds of meters (Harvey and Bencala, 1993; Anderson et al., 2005; Gooseff et al., 2006, Fernald et al. 2006; Kasahara and Hill, 2007). However, this

approach remains site-specific and its results cannot be easily transferred to different locations, but it allows to consider the reciprocal influence of all the key factors affecting surface water-groundwater exchange.

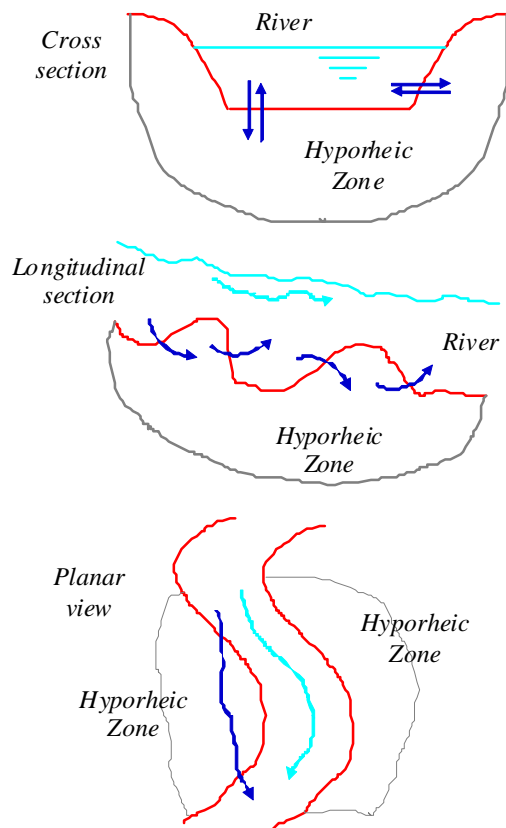


**Figure 1.** Vertical and lateral exchange between surface water and groundwater (after Findlay, 1995).

A second approach studies how the transport of chemicals in streams is influenced by the exchange with the hyporheic zones (Fernald et al., 2001; De Smedt, 2007; Lautz and Siegel, 2007). Thus, the in-stream concentration of a tracer injected into a river were observed at some sampling points and these data were used to calibrate a one-dimensional stream transport model, such as the transient storage model (TSM) (Bencala and Walters, 1983). The calibrated parameters could then be related to the characteristics of the hyporheic zone. However, this approach can identify only the shorter and faster hyporheic paths in the shallower

streambed, whereas no information is provided on the slower transport to the deeper part of the bed.

Finally, the hyporheic exchange can be analyzed both experimentally and numerically at smaller scales. The exchange due to ripples and dunes has in particular been thoroughly studied, since such bedforms are frequently present in rivers (Thibodeaux and Boyle, 1987; Savant et al., 1987; Elliott and Brooks, 1997a, b; Marion et al., 2002; Packman et al., 2004; Meysman et al., 2006; Boano et al., 2007; Bayani-Cardenas and Wilson, 2006, 2007a, b, c; Feng, 2009). A physically-based model (advective pumping model, APM) has been proposed (Elliott, 1990; Elliott and Brooks, 1997b, a) that identifies two basic processes as being responsible for the exchange of solutes with the hyporheic zone: *pumping* and *turnover*. Pumping indicates the water exchange due to gradients of head on the bed surface caused by the separation of the flow behind the bedforms, while turnover denotes the entrapment and release of water in the sediments due to the deposition and scour of the bed. Furthermore, other models considered the exchange of solutes due to turbulent dispersion (Habel et al., 2002), temperature gradients (Carr and Straughan, 2003), wave motion (Habel and Bagtzoglou, 2005), and meander sinuosity (Boano et al., 2006; Bayani-Cardenas, 2008). Despite those many efforts, the study of the hyporheic zones is far from being concluded and needs further studies.

This paper presents some results of numerical simulations carried out to investigate the basic hydrodynamic interactions between the laminar flow in the water column above triangular bedforms and the Darcian flow in the underlying permeable sediments. The interaction between free-fluid flow and the flow within the porous medium was studied considering the characteristics of the separation region in the free fluid and the depth of the interfacial exchange zone.

## 2. Numerical simulations

The analysis of the flow field in a free fluid-porous medium domain was carried out using numerical simulations. Free-fluid flow was simulated by using the well-known mass conservation and momentum balance equations. For a planar, steady-state and incompressible

flow, they are:

$$\frac{\partial u}{\partial x} + \frac{\partial v}{\partial y} = 0 \quad (1)$$

$$\rho \left( u \frac{\partial u}{\partial x} + v \frac{\partial u}{\partial y} \right) = -\frac{\partial p}{\partial x} + \mu \nabla^2 u + F_x \quad (2)$$

$$\rho \left( u \frac{\partial v}{\partial x} + v \frac{\partial v}{\partial y} \right) = -\frac{\partial p}{\partial y} + \mu \nabla^2 v + F_y$$

where in the Navier-Stokes equations,  $\rho$  is fluid density,  $p$  is fluid pressure,  $F_x$  and  $F_y$  are force terms accounting for gravity or other body forces, and  $u$ ,  $v$  are velocity components in the  $x$  and  $y$  directions, respectively.

In the porous medium, the governing equations are again continuity and momentum balance equations. For a planar, steady-state and incompressible flow, continuity equation is Eq. (1), while momentum balance equations in a porous medium are the empirical Darcy's law, which states that the volume averaged velocity field is determined by the pressure gradient, the fluid viscosity and the structure of the porous medium:

$$\begin{aligned} \frac{\mu}{k} u &= -\frac{\partial p}{\partial x} + F_x \\ \frac{\mu}{k} v &= -\frac{\partial p}{\partial y} + F_y \end{aligned} \quad (3)$$

where  $k$  is porous medium permeability [ $L^2$ ], which is a scalar for an isotropic porous medium.

These equations were solved using Multiphysics 3.5a™ modeling package, which is a commercial multiphysics modeling environment (Multiphysics, 2008). Sequential coupling was implemented. Multiphysics first solved Eqs. (1) and (2) for the pressure  $p$  and the velocity vector components  $u$  and  $v$  within the free fluid domain. Then, the calculated pressure distribution along the bed surface was assigned as a Dirichlet boundary condition for the groundwater flow equation and the flow field in the porous medium was solved.

Multiphysics 3.5a™ was applied to the 2D geometry presented in Fig.2, which represents a free fluid-porous medium domain with free fluid and porous medium depth of 0.45 m and 2.0 m, respectively. These sub-domain are separated by a series of five triangular bedforms 1.0 m long and 0.05 m high, with the crest located at 0.9 m. Thus, bedform aspect ratio  $H_{bed\ form}/L$  was 0.04. This value is within the typical range for dunes,

i.e. 0.04÷0.21 (Paarlberg et al., 2007). This bedforms geometry is that used as base case by Bayani-Cardenas and Wilson (2007) in their numerical study.

For the simulations water at 20 °C with density  $\rho=998.16$  Kg/m<sup>3</sup> and dynamic viscosity  $\mu=1.00 \cdot 10^{-3}$  was selected as fluid, while the intrinsic permeability of the porous medium was  $1 \times 10^{-10}$  m<sup>2</sup>, which is in the range for well-sorted coarse sand. Flow conditions were characterized by using a bedform height-based Reynolds number defined as:

$$Re_H = \frac{u_{avg} H_{bed\ form}}{\nu} \quad (4)$$

where  $u_{avg}$  is the average velocity in the free fluid flow. Eleven numerical simulations were carried out using Multiphysics 3.5a™ to investigate the influence on the flow field of the bedform height-based Reynolds number  $Re_H$ . Table 1 lists all the operative conditions.

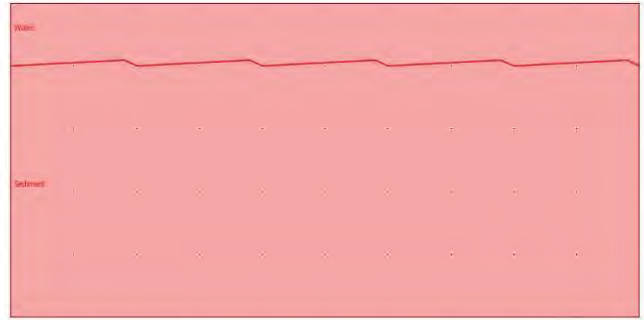


**Figure 2.** The investigated geometry.

Boundary conditions were assigned in both the free-fluid and porous medium sub-domains:

- at the top and the bottom of the water column a no-flow *symmetry* boundary condition and a *no-slip* condition were assigned, respectively;
- at the top boundary of the porous domain a prescribed *pressure* condition was assigned. This pressure was derived solving the Navier-Stokes equations in the above free-fluid domain;
- the lower boundary of the porous domain was considered impermeable;
- to approximate an infinite horizontal domain solution, a spatially *periodic pressure* and *velocity* boundary condition was assigned along the vertical sides for both the water column and the porous

medium. The same mean pressure drop,  $dp$ , was prescribed between the two vertical boundaries for both domains resulting in an ambient flow always from left to right.

Stability and accuracy of the Navier-Stokes solution was ensured via using Lagrange  $p_2-p_1$  elements (second order Lagrange elements for velocity and linear for pressure). Similarly, second order Lagrange elements was used for the Darcian domain.

**Table 1.** Key parameters of the numerical simulations

Run	$dp$ - Pa	$u_{avg}$ - m/s	$Re_H$
1	0.00001	0.00011	6
2	0.00011	0.00120	60
3	0.00033	0.00353	176
4	0.00107	0.01139	569
5	0.00213	0.02250	1123
6	0.00319	0.03344	1669
7	0.00425	0.04455	2224
8	0.00529	0.05532	2761
9	0.00614	0.06411	3200
10	0.00740	0.07718	3852
11	0.00850	0.08850	4417

Different mesh characteristics were tested. After that, different values for the maximum element size were selected for the free fluid, the porous medium and the fluid-porous interface. Maximum elements sizes were 0.025, 0.05 and 0.01 m for the free fluid, the porous medium and the fluid-porous interface, respectively. Overall, the used mesh had 47160 elements, with a minimum *element quality* of 0.664. This parameter is related to the element aspect ratio, which means that anisotropic elements can get a low quality measure even though the element shape is reasonable. It is a scalar from 0 to 1. Mesh quality visualization demonstrated a uniform quality of the elements of the mesh.

About the solver settings, stationary solver was used, where the relative tolerance and the maximum number of segregated iterations were set to  $1.0 \cdot 10^{-6}$  and 50, respectively.

### 3. Numerical results. Discussion

Numerical simulations provided velocity

field and pressure values throughout the flow domain.

The analysis of results was first focused to characterize the flow field close to the sediment-water interface. The flow in the water-column accelerates on the stoss side and decelerates on the lee side of the bedform. A separation region can be observed downstream of the bedform crest with backflow to the crest (Fig.3). Low velocities (blue) were observed in the porous medium and in the separation region.

The separation region became larger with the increasing  $Re_H$  (Fig.4). The eddy detachment point,  $x_d$ , migrates upstream and up the lee face towards the crest, while the reattachment point,  $x_r$ , migrates downstream and up the stoss face.

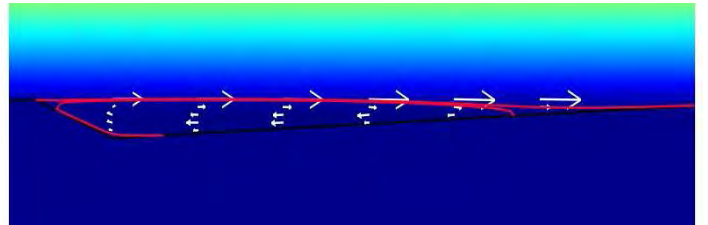


**Figure 3.** The separation region downstream the dune crest for  $Re_H=2224$ .

Fig.4 presents the values of  $L_e/L$  against the bedform height-based Reynolds number  $Re_H$ . Numerical results from Multiphysics 3.5a were successfully compared with those calculated by Bayani-Cardenas and Wilson (2007). At the lowest  $Re_H$  no separation region was observed. The eddy size, measured by length  $L_e=x_r-x_d$ , was particularly sensitive to the current at low  $Re_H$ . Over  $Re_H=1000$  the increase of separation length was slow up to an asymptotic value.

The value and the location of the separation region was closely related to the distribution of the pressure from Navier-Stokes equations at the sediment-water interface since the detachment and reattachment points were located close to the points of minimum and maximum pressure along the bedform. In the bulk water column, mean pressure gradient dominates over local pressure gradients generated by the current-bedform interaction. Note that the pressure was continuous across the sediment-water interface. Below the interface, a backflow region was observed within the porous medium. The area of this region increased with the increasing  $Re_H$  following the pattern observed for  $L_e/L$ . Over

$Re_H=1000$ , two backflow regions were observed. One close to the crest, another one downstream to the dune trough along the stoss face.

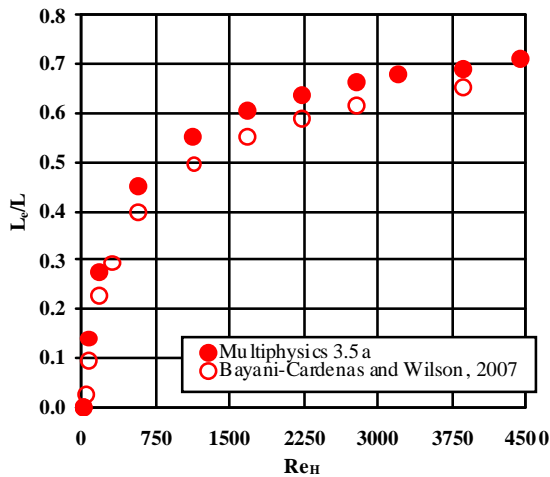


**Figure 4.** Non-dimensional separation length  $L_s/L$  vs  $Re_H$ .

Second, the characteristics of the flow below the sediment-water interface were considered. Fig.5 presents the flow field in the porous medium for  $Re_H=569$ . Note that the velocity vectors (arrows) show only flow direction (not magnitude). Water enter into the bed on the bed on the upper part of the bedform's stoss face, and back up into the water column on the lee face and the lower part of the stoss face. This area is the hyporheic zone or the interfacial exchange zone (Bayani-Cardenas, 2007). Below the hyporheic zone, the mean pressure gradient dominated over local gradients. This results in *underflow*, or ambient flow (Bayani-Cardenas and Wilson, 2007), within the sediments and was present in all the simulations. Note that the mean pressure gradient is the same in both domains.

As already done by Bayani-Cardenas and Wilson (2007), the hyporheic zone was visually identified on a high-density plot of streamlines picking the streamline which separated the sediments region affected by exchange flows with the water column from the unaffected area dominated by underflow. The maximum vertical depth of this zone,  $d_z$ , was defined as the vertical distance from the deepest point of this streamline to the trough of the third bedform. Furthermore, in the hyporheic zone a sub-horizontal exchange

flow between the sediments region below adjacent bedforms was observed.

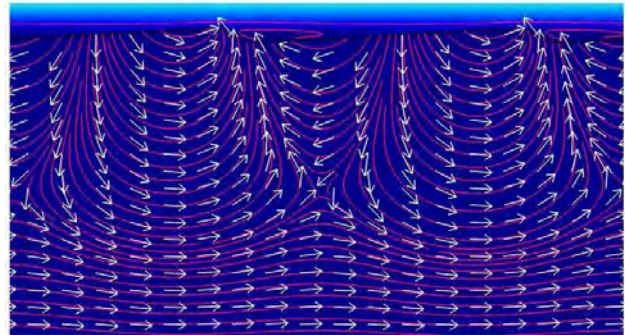


**Figure 5.** Streamline and velocity vectors in the porous medium for  $Re_H=569$ .

As the the bedform height-based Reynolds number  $Re_H$  increased, the depth of the hyporheic zone rapidly increased up to  $Re_H=1000$ . After that,  $d_z$  increased gently towards some asymptotic limit (Fig.6). After all, the depth of the hyporheic zone exhibited the same trend with  $Re_H$  of the length of the separation region downstream the bedform crest. As already pointed out by Bayani-Vardenas and Wilson (2007), this confirmed that the separation region and the related bottom pressures controlled the flow field in the upper part of the porous medium and the size of the hyporheic zone. The  $d_z/L$  data were in close agreement with those from Bayani-Cardenas and Wilson (2007).

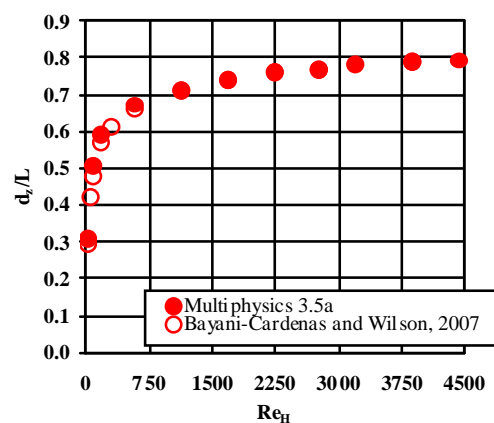


**Figure 6.** Non-dimensional hyporheic zone depth  $d_z/L$  vs  $Re_H$ .

## 7. Conclusions

In recent years, an increasingly attention was addressed to the analysis of the hyporheic zone, where groundwater and stream water are mixing.

The papers presented the results of a numerical study of the flow in a coupled free fluid-porous medium domain. Numerical results confirmed previous numerical studies that have pointed out that the separation region and the related bottom pressures is a key parameter controlling the flow field in the upper part of the porous medium and the size of the hyporheic zone. Also, the numerical results confirmed the role of the bedform height-based Reynolds number of the water column in the evolution of the characteristics of both the separation region and the hyporheic zone.

## 8. References

- Anderson, J.K., Wondzell, S.M., Gooseff, M.N., and Haggerty, R., Patterns in stream longitudinal profiles and implications for hyporheic exchange flow at the H.J. Andrews Experimental Forest, Oregon, USA, *Hydrol. Process.* **19**, 2931–2949 (2005)
- Bayani-Cardenas, M. and Wilson, J.L., The influence of ambient groundwater discharge on exchange zones induced by current–bedform interactions, *Journal of Hydrology*, **331**, 103–109 (2006)
- Bayani-Cardenas, M. and Wilson, J.L., Hydrodynamics of coupled flow above and below a sediment–water interface with triangular bedforms, *Advances in Water Resources*, **30**(1), 301–313 (2007a)
- Bayani-Cardenas, M. and Wilson, J.L., Dunes, turbulent eddies, and interfacial exchange with permeable sediments, *Water Resour. Res.*, **43**(3), (2007b)
- Bayani-Cardenas, M. and Wilson, J.L., Exchange across a sediment–water interface with ambient groundwater discharge, *Journal of Hydrology*, **346**, 69–80 (2007c)
- Bayani-Cardenas, M., The effect of river bend morphology on flow and timescales of surface water–groundwater exchange across pointbars, *Journal of Hydrology*, **362**, 134–141 (2008)
- Bencala, K.E., and Walters, R.A., Simulation of solute transport in a mountain pool-and-riffle stream: a transient storage model, *Water Resour. Res.*, **19**(3), 718–724 (1983)
- Boano, F., Solute transport in rivers and hyporheic zones. PhD Thesis (2006)
- Boano, F., Camporeale, C., Revelli, R., and Ridolfi, L., Sinuosity-driven hyporheic exchange in meandering rivers. *Geophys. Res. Lett.*, **33** (2006)
- Boano, F., Revelli, R., and Ridolfi, L., Bedform-induced hyporheic exchange with unsteady flows. *Adv. Water Resour.*, **30**(1), 148–156 (2007)
- Boulton, A., Findlay, S., Marmonier, P., Stanley, E., and Valett, H., The functional significance of the hyporeic zone in streams and rivers, *Annu.Rev.Ecol. Syst.*, **29**, 59–81 (1998)
- Brunke, M. and Gonser, T., The ecological significance of exchange processes between rivers and groundwater, *Freshwater Biol.*, **37**, 1–33 (1997)
- Dade, W.B., Near-bed turbulence and hydrodynamic control of diffusional mass transfer at sea floor, *Limnol.Oceanogr.*, **38**(1), 52–69 (1993)
- De Smedt, F., Analytical solution and analysis of solute transport in rivers affected by diffusive transfer in the hyporheic zone, *Journal of Hydrology* 339, 29–38 (2007)
- Elliott, A.H., Transport of solutes into and out of stream beds. Rep. No.KH-R-52, W. M. Keck Laboratory of Hydraulics and Water Resources, California Institute of Technology, Pasadena, Calif. (1990)
- Elliott, A.H. and Brooks, N.H., Transfer of nonsorbing solutes to a streambed with bed forms: Theory, *Water Resour. Res.*, **33**(1), 123–136 (1997a)
- Elliott, A.H. and Brooks, N.H., Transfer of nonsorbing solutes to a streambed with bed forms: Laboratory experiments, *Water Resour. Res.*, **33**(1), 137–151 (1997b)
- Feng, Z.G., and Michaelides, E.E., Secondary flow within a river bed and contaminant transport, *Environmental Fluid Mechanics*, **9**(6), 617–634 (2009)
- Fernald, A.G., Landers, D.H., and Wigington, P.J. Jr., Water quality changes in hyporheic flow paths between a large gravel bed river and off-channel alcoves in Oregon, USA, *River Res. Applic.*, **22**, 1111–1124 (2006)
- Fernald, A.G., Wigington, P.J. Jr., and Landers, D.H. (2001). Transient storage and hyporheic flow along the Willamette River, Oregon: Field measurements and model estimates. *Water*

- Resour. Res., **37**(6), 1681–1694 (2001)
- Findlay, S., Strayer, D., Goumbala, C., and Gould, K., Metabolism of streamwater dissolved organic carbon in the shallow hyporheic zone. *Limnol. Oceanogr.*, **38**(7), 1493–1499 (1993)
- Findlay, S., Importance of surface-subsurface exchange in stream ecosystems: The hyporheic zone, *Limnol. Oceanogr.*, **40**(1), 159–164 (1995)
- Gooseff, M.N., Anderson, J.K., Wondzell, S.M., LaNier, J., and Haggerty, R., A modelling study of hyporheic exchange pattern and the sequence, size, and spacing of stream bedforms in mountain stream networks, Oregon, USA, *Hydrol. Process.* **20**, 2443–2457 (2006)
- Habel, F., Mendoza, C., and Bagtzoglou, A.C., Solute transport in open channel flows and porous streambeds. *Advances in Water Resources* **25**, 455–469 (2002)
- Habel, F. and Bagtzoglou, A.C., Wave induced flow and transport in sediment beds. *J. Am. Water Resour. Ass.*, **41**(2), 461–476 (2005)
- Harvey, J.W. and Fuller, C.C., Effect of enhanced manganese oxidation in the hyporheic zone on basin-scale geochemical mass balance. *Water Resour. Res.*, **34**(4), 623–636 (1998)
- Hancock, P., Boulton, A., and Humphreys, W., Aquifers and hyporheic zones: Towards an ecological understanding of groundwater. *Hydrogeol. J.*, **13**, 98–111 (2005)
- Huettel, M., Ziebis, W., Forster, S., and Luther G.W., Advective transport affecting metal and nutrient distributions and interfacial fluxes in permeable sediments, *Geochimica et Cosmochimica Acta*, **62**(4), 613–631 (1998)
- Huettel, M., Røy, H., Precht, E., and Ehrenhauss, S., Hydrodynamical impact on biogeochemical processes in aquatic sediments., *Hydrobiologia*, **494**(3), 231–236, (2003)
- Kasahara, T., and Hill, A.R., Lateral hyporheic zone chemistry in an artificially constructed gravel bar and a re-meandered stream channel, Southern Ontario, Canada, *J. Am. Water Resour. Ass.*, **43**(5), 1257–1269 (2007)
- Lautz, L.L., and Siegel, D.I., The effect of transient storage on nitrate uptake lengths in streams: an inter-site comparison, *Hydrol. Process.* **21**, 3533–3548 (2007)
- Marion, A., Bellinello, M., Guymer, I., and Packman, A., Effect of bed form geometry on the penetration of nonreactive solutes into a streambed. *Water Resour. Res.*, **38**(10), 1209–1221 (2002)
- Meysman, F.J.R., Galaktionov, O.S., Cook, P.L.M., Janssen, F., Huettel, M., and Middleburg, J.J., Quantifying biologically and physically induced flow and tracer dynamics in permeable sediments, *Biogeosciences Discuss.*, **3**, 1809–1858, (2006)
- Multiphysics 3.5a, User's Guide, ComSol AB, Sweden, 2009
- Nishihara, G.N., and J.D. Ackerman, Mass transport in aquatic environments. pp. 299–326 In: C. Gualtieri and D.T. Mihailovic (eds.) *Fluid Mechanics of Environmental Interfaces*. Taylor & Francis (2008)
- Paarlberg, A.J., Dohmen-Janssen, C.M., Hulscher, S.J.M.H., and Termes. P., A parameterization of flow separation over subaqueous dunes, *Water Resour. Res.*, **43**, (2007)
- Packman, A.I., Salehin, M., and Zaramella, M., Hyporheic exchange with gravel beds: Basic hydrodynamic interactions and bedform-induced advective flows., *J. Hydraul. Eng.*, **130**(7), 647–656 (2004)
- Savant, S.A., Reible, D.D., and Thibodeaux, L.J., Convective transport within stable river sediments. *Water Resour. Res.*, **23**(9), 1763–1768 (1987)
- Thibodeaux, L.J. and Boyle, J. D., Bedform-generated convective transport in bottom sediment. *Nature*, **325**(6102):341–343 (1987)
- Wöorman, A., Packman, A.I., and Jonsson, K., Effect of flow-induced exchange in hyporheic zones on longitudinal transport of solutes in streams and rivers. *Water Resour. Res.*, **38**(1), 1001–1016 (2002)